The Astrophysical Journal Letters, 907:L42 (6pp), 2021 February 1 https://doi.org/10.3847/2041-8213/abd413

Discovery of a Candidate Hypervelocity Star Originating from the Sagittarius Dwarf Spheroidal Galaxy

Yang Huang[1], Qingzheng Li[2,3], Huawei Zhang[4,5], Xinyi Li[1], Weixiang Sun[1], Jiang Chang[6,7], Xiaobo Dong[2], and Xiaowei Liu[1]

[1] South-Western Institute for Astronomy Research, Yunnan University, Kunming 650500, People's Republic of China; yanghuang@ynu.edu.cn, x.liu@ynu.edu.cn
[2] Yunnan Observatories, Chinese Academy of Sciences, Kunming 650011, People's Republic of China; liqingzheng@ynao.ac.cn
[3] University of Chinese Academy of Sciences, Beijing 100049, People's Republic of China
[4] Department of Astronomy, School of Physics, Peking University, Beijing 100871, People's Republic of China
[5] Kavli Institute for Astronomy and Astrophysics, Peking University, Beijing 100871, People's Republic of China
[6] Key Lab of Optical Astronomy, National Astronomical Observatories, Chinese Academy of Sciences, Beijing 100012, People's Republic of China
[7] Purple Mountain Observatory, Chinese Academy of Sciences, Nanjing 210034, People's Republic of China
Received 2020 September 11; revised 2020 November 24; accepted 2020 December 16; published 2021 February 2

Abstract

In this Letter, we report the discovery of an intriguing hypervelocity star (HVS; J1443+1453) candidate that is probably from the Sagittarius Dwarf Spheroidal galaxy (Sgr dSph). The star is an old and very metal-poor low-mass main-sequence turn-off star (age ∼14.0 Gyr and [Fe/H] = −2.23 dex) and has a total velocity of $559.01^{+135.07}_{-87.40}$ km s^{-1} in the Galactic rest frame and a heliocentric distance of $2.90^{+0.72}_{-0.48}$ kpc. The velocity of J1443+1453 is larger than the escape speed at its position, suggesting that it is a promising HVS candidate. By reconstructing its trajectory in the Galactic potential, we find that the orbit of J1443+1453 intersects closely with that of Sgr dSph $37.8^{+4.6}_{-6.0}$ Myr ago, when the latter has its latest pericentric passage through the Milky Way. The encounter occurs at a distance $2.42^{+1.80}_{-0.77}$ kpc from the center of Sgr dSph, a distance that is smaller than the size of the Sgr dSph. The chemical properties of this star are also consistent with those of an Sgr dSph-associated globular cluster, or of the Sgr stream member stars. Our finding suggests that J1443+1453 is an HVS that is either tidally stripped from the Sgr dSph or ejected from the Sgr dSph by the gravitational slingshot effect, requiring a (central) massive/intermediate-mass black hole or a (central) massive primordial black hole in the Sgr dSph.

Unified Astronomy Thesaurus concepts: Hypervelocity stars (776); Galaxy kinematics (602); Sagittarius dwarf spheroidal galaxy (1423); Galaxy stellar halos (598); Chemical abundances (224)

1. Introduction

The existence of escaping hypervelocity stars (HVSs) in our Milky Way (MW) was first proposed by Hills (1988) as a consequence of the dynamical interactions between a stellar binary and the central super massive black hole (SMBH). These interactions can propel one member of the binary and accelerate it to a speed exceeding 1000 km s^{-1}, high enough to escape the gravitational potential of our Galaxy. The first HVS, a B-type star with an extreme radial velocity of 709 km s^{-1} in the Galactic rest frame, was discovered serendipitously in a spectroscopic survey of faint blue horizontal-branch (BHB) star candidates in the Galactic halo (Brown et al. 2005). The star, together with two dozen early-type HVSs discovered in the follow-up dedicated surveys (Brown et al. 2006, 2009, 2012, 2014; Zheng et al. 2014; Huang et al. 2017), provide strong support for the Hills mechanism. Most recently, the current fastest HVS was discovered serendipitously by the Southern Stellar Stream Spectroscopic Survey (S^5) with a total velocity of 1755 ± 50 km s^{-1} located at a heliocentric distance of ∼9 kpc (Koposov et al. 2020). By integrating its backward trajectory, this star was found to point unambiguously to the Galactic Center, providing direct evidence to the Hills mechanism.

In addition to the Galactic Center origin, several alternative mechanisms capable of ejecting HVSs have been proposed, including ejected companions of Type Ia supernovae (SNe Ia; Wang & Han 2009) and the result of dynamical interaction between multiple stars (e.g., Gvaramadze et al. 2009). The two mechanisms are supported by the discovery of HVSs US708 (Geier et al. 2015) and HD 271791 (Heber et al. 2008), respectively. Moreover, HVSs could also originate from the MW's satellite galaxy, either by tidally stripping (Abadi et al. 2009) or the gravitational slingshot effect (e.g., Boubert & Evans 2016; García-Bellido 2017; Montanari et al. 2019), assuming that the satellite galaxy hosts a central massive/intermediate-mass black hole or a central massive primordial black hole (PBH). Currently, the HVS HE 0437-5439 is suggested to be ejected from the Large Magellanic Cloud (LMC) through Hills mechanism, requiring a massive black hole with mass of at least 4×10^3–$10^4\ M_\odot$ (Erkal et al. 2019). More recently, Montanari et al. (2019) conducted a systematic search of candidate HVSs ejected due to close encounters between stars and PBHs in the dense environments of dwarf spheroidals, in the Gaia data release 2 (DR2) HVS sample. However, no confident candidates are found.

In this Letter, we report the discovery of a candidate HVS, J1443+1453, that probably originated from the Sagittarius Dwarf Spheroidal galaxy (Sgr dSph). In Section 2, we present the properties of J1443+1453. In Section 3, the possible origins are explored. Finally, we summarize in Section 4.

2. J1443+1453 Properties

2.1. Spectroscopy

J1443+1453 was spectroscopically observed twice, with a short time interval of one week in between, by the Sloan Extension for Galactic Understanding and Exploration survey (SEGUE; Yanny et al. 2009). Heliocentric radial velocities (HRVs) and stellar atmospheric parameters (effective

Table 1
The Measured Parameters of HVS Candidate J1443+1453

Parameter	Value	Units
R.A. (J2000)	14:43:25.76	
Decl. (J2000)	+14:53:36.3	
Gaia DR2 source_id	1186023710910901760	
Gaia DR2 Proper motion $\mu_\alpha \cos\delta$	-46.914 ± 0.121	mas yr^{-1}
Gaia DR2 Proper motion μ_δ	-1.465 ± 0.096	mas yr^{-1}
Gaia DR2 Parallax	0.348 ± 0.065	mas
Gaia DR2 G-band magnitude	16.072 ± 0.002	mag
Gaia DR2 $G_{\rm BP} - G_{\rm RP}$	0.627 ± 0.009	mag
Distance	$2.90^{+0.72}_{-0.48}$	kpc
SDSS g-band magnitude	16.321 ± 0.004	mag
SDSS r-band magnitude	16.066 ± 0.004	mag
Color excess $E(B-V)_{\rm SFD}$	0.016	mag
Heliocentric radial velocity	194.25 ± 1.97	km s^{-1}
Effective temperature $T_{\rm eff}$	6405 ± 130	K
Surface gravity $\log g$	3.64 ± 0.21	dex
Metallicity [Fe/H]	-2.23 ± 0.11	dex
α-element to iron ratio [α/Fe]	0.14 ± 0.10	dex
Galactocentric distance $r_{\rm GC}$	$7.30^{+0.31}_{-0.34}$	kpc
Total velocity $V_{\rm GSR}$	$559.01^{+135.07}_{-87.40}$	km s^{-1}
Age	$14.0^{+0.5}_{-2.0}$	Gyr
Mass	$0.75^{+0.03}_{-0.01}$	$M_\odot$

temperature $T_{\rm eff}$, surface gravity $\log g$, and metallicity [Fe/H]) derived with the SEGUE Stellar Parameter Pipeline (SSPP; Lee et al. 2008a) from the two spectra are almost identical and their final weighted means (by measurement errors) are presented in Table 1 (the uncertainties listed here are typical values yielded by SSPP; Lee et al. 2008b, 2011). It was an F-type ($T_{\rm eff} = 6405$ K) star with a very low metallicity ([Fe/H] $= -2.23$). The measured HRV 194.25 ± 1.97 km s^{-1} corresponds to a Galactic rest-frame radial velocity of 228.22 ± 1.97 km s^{-1}. The average SEGUE spectrum (weighted mean by flux uncertainties) of J1443+1453 is shown in the left panel of Figure 1. For comparison, a synthetical spectrum taken from the Göttingen spectral library (Husser et al. 2013) of atmospheric parameters similar to those of J1443+1453 as derived from the SEGUE spectra is overplotted, showing the robustness of the derived atmospheric parameters.

2.2. Astrometry

Apart from the spectroscopic observations, accurate astrometric measurements are available for J1443+1453 from the Gaia DR2 (Gaia Collaboration et al. 2018; Lindegren et al. 2018). We estimate the distance to J1443+1453 from the Gaia parallax with a Bayesian approach

$$P(d|\varpi, \sigma_\varpi) \propto P(\varpi|d, \sigma_\varpi) \times d^2 P(r_{\rm GC}). \quad (1)$$

Here, the parallax likelihood is given by

$$P(\varpi|d, \sigma_\varpi) = \frac{1}{\sqrt{2\pi}\,\sigma_\varpi} \exp \frac{-\left(\varpi - \varpi_{\rm ZP} - \frac{1}{d}\right)^2}{2\sigma_\varpi^2}, \quad (2)$$

where $\varpi_{\rm ZP}$ is the zero-point of the Gaia DR2 parallax and we adopt a value of -0.048 mas as determined statistically recently (Schönrich et al. 2019). We set the density prior $P(r_{\rm GC}) \propto r_{\rm GC}^{-3.39}$ (McMillan et al. 2018), given the halo-star nature of J1443+1453. A distance of $2.90^{+0.72}_{-0.48}$ kpc is deduced for J1443+1453.

Combing the distance derived above and the celestial coordinates, proper motions from the Gaia DR2 and HRV from the SEGUE, the 3D position and velocity of J1443+1453 are further derived. To do so, we adopt the Galactocentric distance of the Sun, $R_0 = 8.178$ kpc, as measured by the Gravity Collaboration (Gravity Collaboration et al. 2019), and vertical displacement of the Sun from the disk mid-plane, $Z_\odot = 25$ pc (Bland-Hawthorn & Gerhard 2016). The Solar motions with respect to the local standard of rest adopted here are $(U_\odot, V_\odot, W_\odot) = (7.01, 10.13, 4.95)$ km s^{-1} (Huang et al. 2015). For the circular speed at the Solar position V_c (R_0), we use a value of 225 km s^{-1}, in concordance with the recent measurements (Bovy et al. 2012; Huang et al. 2016; Bland-Hawthorn & Gerhard 2016). The errors of the resultant 3D position and velocity are all derived by Monte Carlo (MC) simulations, by sampling the observational uncertainties of HRV from the SEGUE, proper motions from the Gaia DR2 and the distance posterior probability distribution function (PDF) derived above. The 3D position and velocity of J1443+1453 thus deduced in a right-handed Galactocentric Cartesian coordinate system are, respectively $(X, Y, Z) = (-6.82^{+0.32}_{-0.22}, 0.32^{+0.08}_{-0.05}, 2.57^{+0.60}_{-0.42})$ kpc and $(V_X, V_Y, V_Z) = (-292.29^{+60.34}_{-98.74}, -183.39^{+74.27}_{-111.42}, 439.80^{+67.45}_{-41.21})$ km s^{-1}. The upper and lower uncertainties correspond to the 16% and 84% percentiles of the final PDF yielded by the MC simulations. Here X passes through the Sun and points toward the Galactic center, Y is in the direction of the Galactic rotation and Z points toward the north Galactic pole.

The above results show that J1443+1453 has a total velocity in the Galactic rest frame $V_{\rm GSR}$ of $559.01^{+135.07}_{-87.40}$ km s^{-1}, and locates at a Galactocentric distance $r_{\rm GC}$ of $7.3^{+0.31}_{-0.34}$ kpc. The velocity is larger than the escape speed measured directly (Williams et al. 2017) or predicted by the potential models of the MW (Bovy 2015; Huang et al. 2016) at $r_{\rm GC} = 7.3$ kpc, placing J1443+1453 a HVS candidate[8] (see the right panel of Figure 1).

2.3. Age and Mass

The age and mass of J1443+1453 are derived again by a Bayesian approach, based on the observational constraints and stellar isochrones taken from the Dartmouth Stellar Evolution Program (DSEP; Dotter et al. 2008). The observational constraints include the metallicity derived from the SEGUE spectra, the photometric colors from the Sloan Digital Sky Survey (SDSS) imaging survey (after corrected for the dust reddening from Schlegel et al. 1998) and the r-band absolute magnitude inferred from the distance deduced above and the SDSS photometry (again corrected for the dust reddening). In the estimation, the PDF of the parameters to be determined is assumed to have the form

$$f(\tau, M) = NP(\tau, M)L(\tau, M), \quad (3)$$

where N is a normalization factor to ensure $\int\int f(\tau, M)d\tau dM = 1$. P (τ, M) represents the priors on age and mass, and we have adopted a uniform prior for the age and a Salpeter initial mass function (Salpeter 1955) for the mass. The likelihood function L is given by

$$L = \prod_{i=1}^{n} \frac{1}{\sqrt{2\pi}\,\sigma_i} \times \exp(-\chi^2/2), \quad (4)$$

[8] Considering the measured total velocity uncertainty, J1443+1453 also has 43% possibility of being a bound star, if adopting the escape velocity curve from Williams et al. (2017).

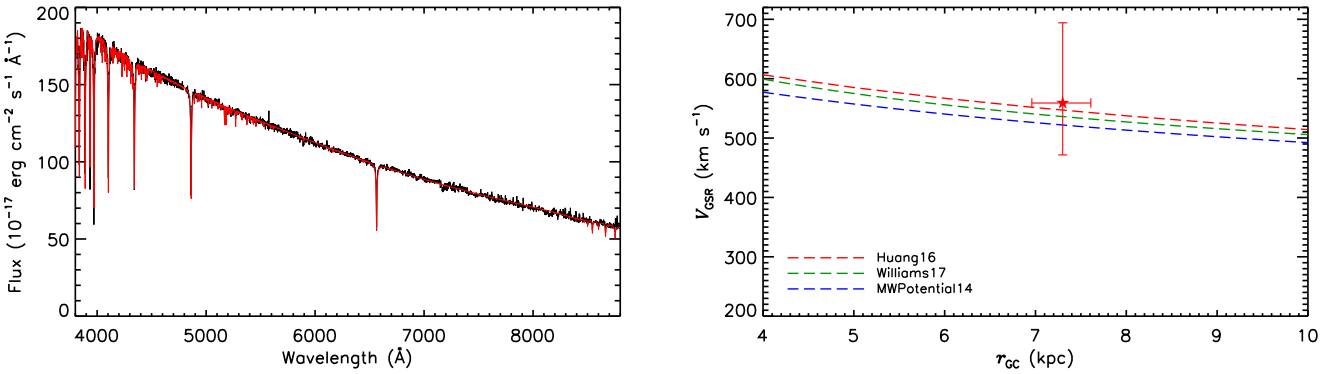

Figure 1. Left panel: average spectrum of J1443+1453 from the SUGUE survey. A synthetical spectrum (in red) of $T_{\rm eff} = 6500$ K, $\log g = 4.0$ dex, [Fe/H] $= -2.0$ dex, and [α/Fe] $= 0.20$ dex, is overplotted for comparison. Right panel: the Galactic rest-frame total velocity of J1443+1453 compared with the escape velocity curves, either derived directly (green dashed line; Williams et al. 2017) or predicted by the Galactic potential models (red and blue dashed lines; Bovy 2015; Huang et al. 2016).

where

$$\chi^2 = \sum_i^n \left(\frac{O_i - P_i(\tau, M)}{\sigma_i} \right)^2. \quad (5)$$

Here O denotes the aforementioned observational constraints and P denotes the values given by the isochrone for given τ and M. A constant value 0.20 dex of α-element to iron abundance ratio [α/Fe], close to that measured for J1443+1453, is adopted for all the isochrones. The above analysis yields a mass of $0.75^{+0.03}_{-0.01}$ $M_\odot$ and an almost cosmic age of $14.0^{+0.5}_{-2.0}$ Gyr for J1443+1453, where the values and the uncertainties correspond to the 50%, and the 16% and 84% percentiles of the resultant posterior PDF yielded by the Bayesian approach. To show the robustness of the results, we compare the position of J1443+1453 with isochrone of [Fe/H] $= -2.0$ dex, [α/Fe] $=$ 0.20 dex and $\tau = 14.0$ Gyr in the M_r versus $(g - r)_0$ plane in Figure 2. An empirical isochrone (An et al. 2008) of globular cluster NGC 5466 ($d = 16.0$ kpc, [Fe/H] $= -1.98$ dex and $\tau = 13.0 \pm 0.75$ Gyr; Harris 2010; Dotter et al. 2010) is also overplotted. The plot shows that J1443+1453 falls closely near the main-sequence turn-off (MSTO) region, for both the theoretical and the empirical isochrones.

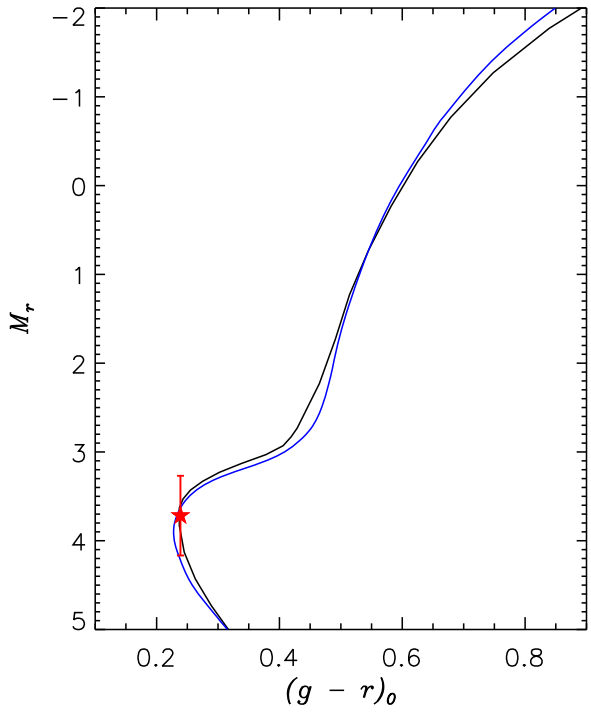

Figure 2. Color-absolute magnitude diagram for J1443+1453 (red star). The black line represents an empirical isochrone of globular cluster NGC 5466. The blue line represents a theoretical isochrone (with [Fe/H] $= -2.0$ dex, [α/Fe] $= 0.20$ dex, and $\tau = 14.0$ Gyr) taken from the Dartmouth Stellar Evolution Program (Dotter et al. 2008).

3. The Possible Origins of J1443+1453

3.1. Backward Orbit Analysis

To constrain the possible ejection location of J1443+1453, we perform a backward orbital integration in a model Galactic potential with the package `Gala` (Price-Whelan 2017). We use the classical Galactic potential model `MWPotential2014` (Bovy 2015) consisting of three components, a bulge, a disk, and a dark matter halo. The orbit is integrated backward in time step of 0.1 Myr. A representation of the integrated orbit in 3D space is shown in Figure 3(a). We first check if this HVS was ejected by the central SMBH of the MW. We find that J1443 +1453 intersects the Galactic plane ($Z = 0$ kpc) $5.6^{+0.4}_{-0.6}$ Myr ago at location (X, Y) $= (-5.07^{+1.04}_{-0.73}, 1.34^{+0.80}_{-0.51})$ kpc (see Figure 3(b)). The intersection is thus too far from the Galactic center to make it an HVS created by the Hills Mechanism.

To further explore the possible origin of J1443+1453, we integrate the backward trajectories of 150 Galactic globular clusters and 39 dwarf galaxies with full information of phase-space positions and motions (Fritz et al. 2018; Vasiliev 2019). Here the orbit is integrated up to 5 Gyr back in time with a step of 0.1 Myr. We note that the gravitational influence of the globular cluster or dwarf galaxy is ignored in our orbital analysis. The possible link of the trajectory of J1443+1453 and those of the globular clusters and dwarf galaxies are investigated by sorting the closest orbital distance to half-light/mass–radius ratio (see Table 2 for the top three systems). Excitingly, our backward orbital analysis shows that the orbit of J1443+1453 intersects with that of Sgr dSph within its half-light radius $r_{\rm h} = 2.59$ kpc (McConnachie 2012) $37.8^{+4.6}_{-6.0}$ Myr ago. The closest encounter occurred at an impact distance $2.42^{+1.80}_{-0.77}$ kpc from the core of Sgr dSph. Moreover, the encounter occurred when the Sgr dSph was at position (X, Y, Z) $= (7.37^{+1.74}_{-1.39}, 3.77^{+0.79}_{-0.72}, -13.76^{+1.54}_{-1.44})$ kpc, very close to the

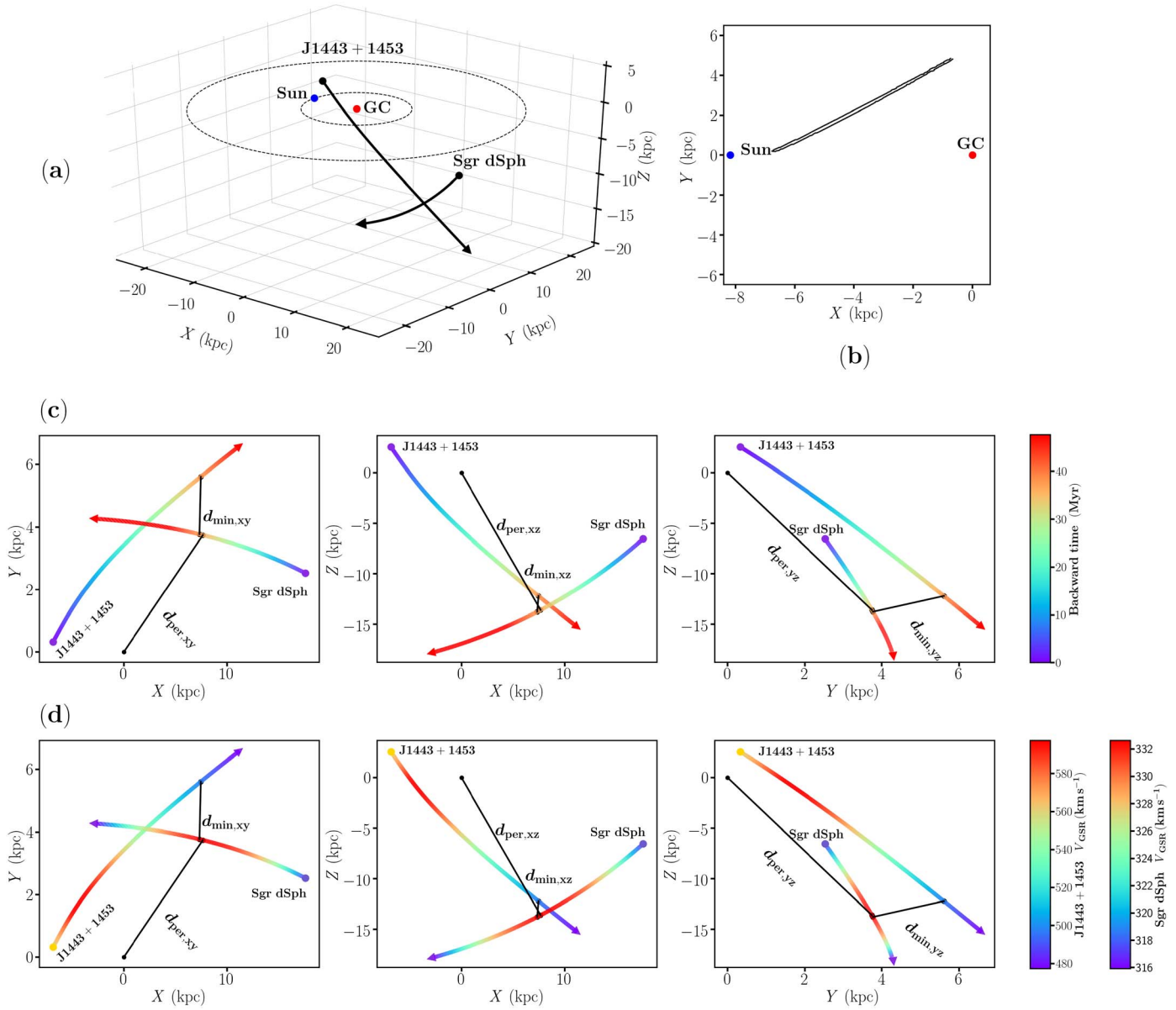

Figure 3. Panel (a): 3D representation of the backward orbits of J1443+1453 and the Sgr dSph. The arrows indicate the directions of the backward orbits. The blue and red dots represent the positions of the Sun and the Galactic Center. The Solar circle ($R = 8.178$ kpc) and the edge of the MW disk ($R = 25$ kpc) are marked by the inner and outer dotted gray lines, respectively. Panel (b): Density of simulated trajectories (black contour = 90% confidence region) where J1443+1453 crosses the Galactic plane, in Cartesian coordinates. The blue and red dots again represent the positions of the Sun and the Galactic Center. Panel (c): 3D orbits of J1443+1453 and the Sgr dSph, projected in *X*–*Y*, *Y*–*Z*, and *X*–*Z* planes and color coded by the backward time as indicated by the right colorbar. In each sub-panel, two black solid lines are drawn, one linking the Galactic Center and the pericenter of Sgr dSph, and another linking J1443+1453 and the Sgr dSph core when the backward integrated orbits of the two intersect at the closest point. Panel (d): the same as Panel (c) but color coded by the total velocities in the Galactic rest-frame of J1443+1453 and the Sgr dSph as indicated by the right colorbars.

pericenter $(X,\ Y,\ Z) = (7.70^{+1.63}_{-1.63},\ 3.74^{+0.61}_{-0.65},\ -13.58^{+0.74}_{-0.60})$ kpc (see Figures 3(c) and (d)) during its latest passage of the MW. At the closest approach, J1443+1453 had a velocity of $689.69^{+103.53}_{-64.72}$ km s^{-1} relative to the Sgr dSph (see Figure 3(d)).

In the current backward orbital analysis, J1443+1453 is 0.97 kpc away from the center of Sgr dSph, during the closest encounter, at 3σ confidence. Even considering the gravitational influence of Sgr dSph (assuming Sgr dSph as a $10^9\,M_\odot$ Keplerian flyby; Erkal & Belokurov 2015), the effect on estimating the closest encounter distance is smaller than 0.2 kpc.

We repeat the whole orbit integration analysis by adopting alternative assumptions to test the robustness of our results. First, we change the Solar motions to $(U_\odot,\ v_\odot,\ W_\odot) = (11.10,\ 250.00,\ 7.24)$ km s^{-1} (Schönrich et al. 2010; Schönrich 2012) and keep other parameters unchanged. The orbit of J1443+1453 intersects with that of the Sgr dSph within its half-light radius $37.8^{+4.6}_{-5.9}$ Myr ago. The closest encounter is $2.52^{+1.89}_{-0.72}$ kpc away from the Sgr dSph core and just around its pericenter. As another test, we change to the default Galactic potential model of `Gala` that consists of four components (nucleus, bulge, disk, and dark matter halo) and again keep other parameters unchanged. Again, J1443+1453 had a close meet with the Sgr dSph at a distance of $2.40^{+1.83}_{-0.69}$ kpc from the core of the latter, $37.2^{+4.4}_{-5.6}$ Myr ago. The tests show that the impact of

Table 2
Top Three Systems Sorted by the Value of $d_{\rm min}/r_h$ (from Small to Large) in the Backward Orbital Analysis of J1443+1453

Name	Closest Distance ($d_{\rm min}$) (kpc)	Backward Time (Myr)	Half-light Radius (r_h) (kpc)	$d_{\rm min}/r_h$
Sgr dSph	2.42	37.8	2.59[a]	0.93
Tucana II	16.45	291.2	0.17[b]	96.76
Ursa Major II	34.08	3.4	0.15[a]	228.73

Notes.
[a] McConnachie (2012).
[b] Koposov et al. (2015).

alternative assumptions on the above orbital analysis is quite limited.

The upper and lower uncertainties of those reported parameters from our orbital analysis come from 16% and 84% percentiles of the PDF yielded by 10,000 MC trajectory calculations, assuming that the measurement errors are normally distributed except the distance (for which the posterior PDF derived above is used directly).

3.2. Chemical Abundances

We show J1443+1453 in the [Fe/H] versus [α/Fe] plane in Figure 4. The location is consistent with the distribution of the Sgr stream member stars and differs significantly from that of the Galactic field stars (Venn et al. 2004). Member stars of the Sgr stream are taken from an analysis based on the LAMOST K giants (Yang et al. 2019). Their elemental abundance ratios have been obtained by applying a data-driven Payne approach to the LAMOST low-resolution spectra (Xiang et al. 2019) of signal-to-noise rations greater than 25 in g-band. More interestingly, the chemical composition of J1443+1453 is very close to globular cluster Terzan 7, known to be associated with the Sgr dSph. The result suggests that J1443+1453 could come from a halo star of the Sgr dSph, in line with the above conclusion from the orbital analysis.

3.3. Origin of J1443+1453

The above orbital and chemical analysis strongly suggested J1443+1453 is originated from the Sgr dSph. Here we discuss the possible ejection mechanisms of J1443+1453 from the Sgr dSph.

First, HVSs could be ejected from disrupting dwarf galaxies by tidally stripping during the pericentric passage of the latter trough the MW (Abadi et al. 2009). The backward orbit analysis shows that the orbit of J1443+1453 intersects closely with that of the Sgr dSph $37.8^{+4.6}_{-6.0}$ Myr ago, when the latter has its latest pericentric passage through the MW. This finding is in excellent agreement with the theoretical prediction by Abadi et al. (2009), and strongly suggests that J1443+1453 is an HVS probably stripped from the tidally disrupting Sgr dSph. As a next step, further numerical simulation is required to investigate the possibility of ejecting J1443+1453 like HVS from the Sgr dSph by tidally stripping.

On the other hand, J1443+1453 can also be ejected from the Sgr dSph by the gravitational slingshot effect (e.g., Hills 1988; García-Bellido 2017; Montanari et al. 2019), if the later is confirmed to host a (central) massive/intermediate-mass black hole or a (central) massive PBH. By assuming the Hills mechanism (Hills 1988; Bromley et al. 2006), the mass of the black hole is at least $1.56^{+2.05}_{-0.70} \times 10^3\,M_\odot$ to eject a HVS like J1443+1453 from the Sgr dSph with an ejection velocity of $689.69^{+103.53}_{-64.72}$ km s^{-1}.

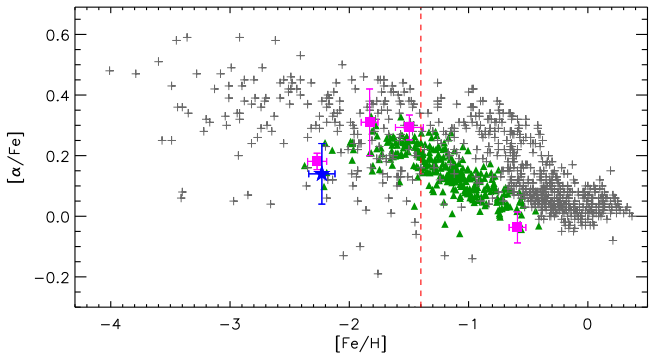

Figure 4. [α/Fe] abundance ratios as a function of [Fe/H] for J1443+1453 (blue star), Sgr dSph-associated globular clusters (magenta squares), Sgr stream member stars (green triangles), and field stars of the Milk Way (gray pluses). The red dashed line marks the rough position of the α-element "knee" of the Sgr stream. The four globular clusters associated with the Sgr dSph are M 54, Terzan 7, Terzan 8, and Arp 2, respectively. Their elemental abundance ratios are all taken from the results based on high-resolution spectroscopy (Sbordone et al. 2005; Carretta et al. 2010, 2014; Mottini et al. 2008).

4. Summary

In this Letter, we present an intriguing HVS (J1443+1453) candidate with a total velocity of $559.01^{+135.07}_{-87.40}$ km s^{-1} in the Galactic rest frame and a heliocentric distance of $2.90^{+0.72}_{-0.48}$ kpc. By backward orbit analysis, this HVS is found to have a close encounter with the Sgr dSph $37.8^{+4.6}_{-6.0}$ Myr ago, during the latest Galactic pericentric passage of the latter. The chemical properties of J1443+1453 also show it could be a member star of the Sgr dSph. These results strongly suggest that J1443+1453 is probably a halo HVS stripped from the tidally disrupting Sgr dSph during its latest pericentric passage, exactly in line with the theoretical predictions (Abadi et al. 2009). On the other hand, we cannot rule out the possibility that this HVS is ejected from the Sgr dSph by the gravitational slingshot effect (e.g., Hills 1988; García-Bellido 2017) by assuming a (central) massive/intermediate-mass black hole or a (central) massive PBH in the Sgr dSph.

We are excited by the prospect of finding more dwarf galaxy-originated HVSs with the ongoing and forthcoming large-scale surveys. Further identifications of such objects will provide not only vital constraints on the nature and ejection mechanisms of HVSs, but also new insights for understanding galaxy formation and evolution.

We would like to thank the referee for their helpful comments. This work is supported by National Key R&D Program of China No. 2019YFA0405500 and National Natural Science Foundation of China grants 11903027, 11833006, 11973001, and U1731108. Y.H. is supported by the Yunnan University grant C176220100006. We used data from the European Space Agency mission Gaia (http://www.cosmos.esa.int/gaia), processed by the Gaia Data Processing and Analysis Consortium (DPAC; see http://www.cosmos.esa.int/web/gaia/dpac/consortium). We also used the data from the SDSS survey.

ORCID iDs

Yang Huang https://orcid.org/0000-0003-3250-2876
Huawei Zhang https://orcid.org/0000-0002-7727-1699
Xiaowei Liu https://orcid.org/0000-0003-1295-2909

References

Abadi, M. G., Navarro, J. F., & Steinmetz, M. 2009, ApJL, 691, L63
An, D., Johnson, J. A., Clem, J. L., et al. 2008, ApJS, 179, 326
Bland-Hawthorn, J., & Gerhard, O. 2016, ARA&A, 54, 529
Boubert, D., & Evans, N. W. 2016, ApJL, 825, L6
Bovy, J. 2015, ApJS, 216, 29
Bovy, J., Allende Prieto, C., Beers, T. C., et al. 2012, ApJ, 759, 131
Bromley, B. C., Kenyon, S. J., Geller, M. J., et al. 2006, ApJ, 653, 1194
Brown, W. R., Geller, M. J., Kenyon, S. J., et al. 2005, ApJL, 622, L33
Brown, W. R., Geller, M. J., Kenyon, S. J., et al. 2006, ApJ, 647, 303
Brown, W. R., Geller, M. J., & Kenyon, S. J. 2009, ApJ, 690, 1639
Brown, W. R., Geller, M. J., & Kenyon, S. J. 2012, ApJ, 751, 55
Brown, W. R., Geller, M. J., & Kenyon, S. J. 2014, ApJ, 787, 89
Carretta, E., Bragaglia, A., Gratton, R. G., et al. 2010, A&A, 520, A95
Carretta, E., Bragaglia, A., Gratton, R. G., et al. 2014, A&A, 561, A87
Dotter, A., Chaboyer, B., Jevremović, D., et al. 2008, ApJS, 178, 89
Dotter, A., Sarajedini, A., Anderson, J., et al. 2010, ApJ, 708, 698
Erkal, D., & Belokurov, V. 2015, MNRAS, 450, 1136
Erkal, D., Boubert, D., Gualandris, A., et al. 2019, MNRAS, 483, 2007
Fritz, T. K., Battaglia, G., Pawlowski, M. S., et al. 2018, A&A, 619, A103
Gaia Collaboration, Brown, A. G. A., Vallenari, A., et al. 2018, A&A, 616, A1
García-Bellido, J. 2017, JPhCS, 840, 012032
Geier, S., Fürst, F., Ziegerer, E., et al. 2015, Sci, 347, 1126
Gravity Collaboration, Abuter, R., Amorim, A., et al. 2019, A&A, 625, L10
Gvaramadze, V. V., Gualandris, A., & Portegies Zwart, S. 2009, MNRAS, 396, 570
Harris, W. E. 2010, arXiv:1012.3224
Heber, U., Edelmann, H., Napiwotzki, R., Altmann, M., & Scholz, R.-D. 2008, A&A, 483, L21
Hills, J. G. 1988, Natur, 331, 687
Huang, Y., Liu, X.-W., Yuan, H.-B., et al. 2015, MNRAS, 449, 162
Huang, Y., Liu, X.-W., Yuan, H.-B., et al. 2016, MNRAS, 463, 2623
Huang, Y., Liu, X.-W., Zhang, H.-W., et al. 2017, ApJL, 847, L9
Husser, T.-O., Wende-von Berg, S., Dreizler, S., et al. 2013, A&A, 553, A6
Koposov, S. E., Belokurov, V., Torrealba, G., et al. 2015, ApJ, 805, 130
Koposov, S. E., Boubert, D., Li, T. S., et al. 2020, MNRAS, 491, 2465
Lee, Y. S., Beers, T. C., Allende Prieto, C., et al. 2011, AJ, 141, 90
Lee, Y. S., Beers, T. C., Sivarani, T., et al. 2008a, AJ, 136, 2022
Lee, Y. S., Beers, T. C., Sivarani, T., et al. 2008b, AJ, 136, 2050
Lindegren, L., Hernández, J., Bombrun, A., et al. 2018, A&A, 616, A2
McConnachie, A. W. 2012, AJ, 144, 4
McMillan, P. J., Kordopatis, G., Kunder, A., et al. 2018, MNRAS, 477, 5279
Montanari, F., Barrado, D., & García-Bellido, J. 2019, MNRAS, 490, 5647
Mottini, M., Wallerstein, G., & McWilliam, A. 2008, AJ, 136, 614
Price-Whelan, A. M. 2017, JOSS, 2, 388
Salpeter, E. E. 1955, ApJ, 121, 161
Sbordone, L., Bonifacio, P., Marconi, G., Buonanno, R., & Zaggia, S. 2005, A&A, 437, 905
Schlegel, D. J., Finkbeiner, D. P., & Davis, M. 1998, ApJ, 500, 525
Schönrich, R. 2012, MNRAS, 427, 274
Schönrich, R., Binney, J., & Dehnen, W. 2010, MNRAS, 403, 1829
Schönrich, R., McMillan, P., & Eyer, L. 2019, MNRAS, 487, 3568
Vasiliev, E. 2019, MNRAS, 484, 2832
Venn, K. A., Irwin, M., Shetrone, M. D., et al. 2004, AJ, 128, 1177
Wang, B., & Han, Z. 2009, A&A, 508, L27
Williams, A. A., Belokurov, V., Casey, A. R., et al. 2017, MNRAS, 468, 2359
Xiang, M., Ting, Y.-S., Rix, H.-W., et al. 2019, ApJS, 245, 34
Yang, C., Xue, X.-X., Li, J., et al. 2019, ApJ, 886, 154
Yanny, B., Rockosi, C., Newberg, H. J., et al. 2009, AJ, 137, 4377
Zheng, Z., Carlin, J. L., Beers, T. C., et al. 2014, ApJL, 785, L23